

Photocurrent Generation in Multilayer Self-Assembly Films Fabricated from Water-Soluble Poly(phenylene vinylene)

Hongmei Li, Yuliang Li,* Jin Zhai, Guanglei Cui, Huibiao Liu, Shengqiang Xiao, Yang Liu, Fushen Lu, Lei Jiang, and Daoben Zhu*^[a]

Abstract: A novel, water-soluble, cationic PPV derivative poly{(2,5-bis(3-bromotrimethylammoniopropoxy)-phenylene-1,4-divinylene)-*alt*-1,4-(2,5-bis(2-(2-hydroxyethoxy)ethoxy))phenylene vinylene} (BH-PPV) has been synthesized by a Heck coupling reaction. Multilayered assemblies of the BH-PPV and the sodium salt of hexa(sulfo-butyl)fullerenes (C₆₀-HS) were fabricated successfully by an alternate depo-

sition technique. The multilayer structures were studied by UV/Vis spectroscopy, small angle X-ray diffraction, and atomic force microscopy. The photoinduced charge transfer property of the self-assembled multilayer film was

Keywords: electron transfer • electrostatic interactions • photocurrent response • polymers • self-assembly

also measured by a three-electrode cell technique. A steady and rapid cathodic 5.5 $\mu\text{A cm}^{-2}$ photocurrent response was measured as the irradiation of the multilayer film was switched on and off. Importantly, the response of on/off cycling is prompt and reproducible. A possible mechanism for the electron-transfer process is proposed.

Introduction

Incorporation of molecular components for light harvesting and charge separation into artificial photosynthetic systems is of great interest from both a fundamental and a practical point of view.^[1] The photosynthetic component includes both the light-harvesting complex and the reaction-center complex, which are coupled to capture solar energy and convert it into chemical energy.^[2] Photoinduced electron transfer has so far been studied extensively using donor-acceptor linked molecules or equivalents.^[3] It is essential to construct appropriate assemblies of these molecules to convert the charge-separated state into chemical or electrical energy in macroscopic quantities. To extract the energy of a charge-separated state in a useful fashion, efforts have been devoted to the spatial organization of the molecules on solid supports, such as lipid bilayer membranes,^[4] sol-gel glasses,^[5] and polyelectrolytes.^[1a,b] Langmuir-Blodgett films^[6] and self-assembly techniques^[7] have been successfully used in photosynthesis-mimicking systems. Using self-assembly methods,

it has been possible to organize molecules into stable lamellar structures on various solid supports. This has resulted in efficient artificial photosynthetic systems that combined the advantages of molecular systems with those of solid-supported systems.^[8]

Recently, increasing interest has been focused on the preparation of uniform, ultrathin organic films by the layer-by-layer deposition technique.^[9] This technique has developed rapidly because it is simple in procedure, easy to automate, and friendly to the environment.^[10] It has become one of the most promising ways to fabricate a controllable molecular array for efficient energy and electron transfer and to construct devices such as photoelectrochemical cells for use in solar energy conversion.^[11] Multilayer film formation has been studied for a range of adsorbate systems, including combinations of cationic and anionic polyelectrolytes^[12] and polyelectrolytes and oppositely charged particles,^[13] or inorganic materials.^[14]

Photo-induced electron transfer in organic optoelectronic systems has been extensively investigated.^[15] Evidence for photoinduced electron transfer from the excited state of a conducting polymer onto fullerene (C₆₀) has been reported by Sariciftci et al.^[16] This evidence provided a molecular approach to high-efficiency photovoltaic conversion and opened a viable way to the use organic materials such as fullerenes and conjugated polymers in applications traditionally reserved for inorganic semiconductors and metals.^[17] Some fullerene-containing films have been fabricated,^[18] poly(phenylene vinylene) (PPV) blended with C₆₀ or modi-

[a] Prof. Y. Li, Prof. D. Zhu, Dr. H. Li, Dr. J. Zhai, Dr. G. Cui, Dr. H. Liu, Dr. S. Xiao, Dr. Y. Liu, Dr. F. Lu, Prof. L. Jiang
Center for Molecular Sciences
Institute of Chemistry
The Chinese Academy of Sciences, Beijing, 100080 (China)
Fax: (+86)10-82616576
E-mail: ylli@iccas.ac.cn

Supporting information for this article is available on the WWW under <http://www.chemeurj.org/> or from the author.

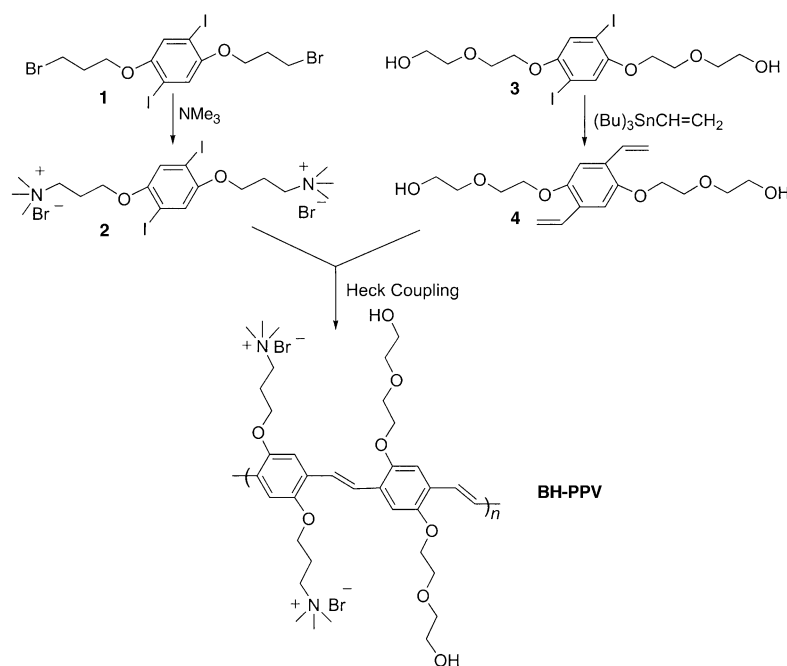
fied C_{60} has attracted the attention of many different research groups. In these systems, the rich and extensive absorption features of PPV guarantee increased absorption cross-sections and an efficient use of the solar spectrum.^[19] In addition, fullerene C_{60} holds great promise as an electron acceptor in electron transfer reactions, which improves the light-induced charge-separation.^[20] However, the drawback is that the C_{60} tends to crystallize, which makes the donor and acceptor molecules incompatible and inclined to phase separation. This results in poor homogeneity and low optical quality of the films. These problems can be overcome if a layer-by-layer self-assembly technique is used to fabricate films. This method has been applied to making organic and hybrid organic/inorganic light-emitting devices by Rubner and co-workers.^[21] In their studies, they used the technique of layer-by-layer sequential adsorption to fabricate heterostructure devices made of PPV and C_{60} . These self-assembled films had to undergo a thermal treatment under dynamic vacuum in order to convert the pPPV (PPV precursor to the conjugated form of PPV) to PPV. Recently, Rubner fabricated bilayer-block devices made of PPV/poly(acrylic acid) and C_{60} /poly(allyl amine hydrochloride), which serve as the electron donor and electron acceptor, respectively.^[22] Upon illumination with a laser beam, the devices showed large photoresponses (current and voltage) that resulted from a photoinduced electron transfer between the PPV and the C_{60} .

Synthetic strategies toward fullerene derivatives that are able to self-assemble with suitably designed conjugated polymers should be considered. In this article, we report the synthesis and characterization of a novel, water-soluble, cationic PPV derivative poly{(2,5-bis(3-bromotrimethylammonio-propoxy)-phenylene-1,4-divinylene)-*alt*-1,4-(2,5-bis(2-(2-hydroxyethoxy)ethoxy))phenylene vinylene} (BH-PPV). We would also like to report the photoinduced charge-transfer properties of self-assembled multilayer films consisting of water-soluble PPV as the electron-donating layer and fullerene with the sulfonate functionality as the electron-accepting layer. A possible mechanism for the electron transfer process is proposed.

Results and Discussion

Polymer synthesis and characterization: Scheme 1 outlines the general approach to the water-soluble cationic poly(phenylene vinylene) (PPV). In this study, 1,4-diiodo-2,5-di-

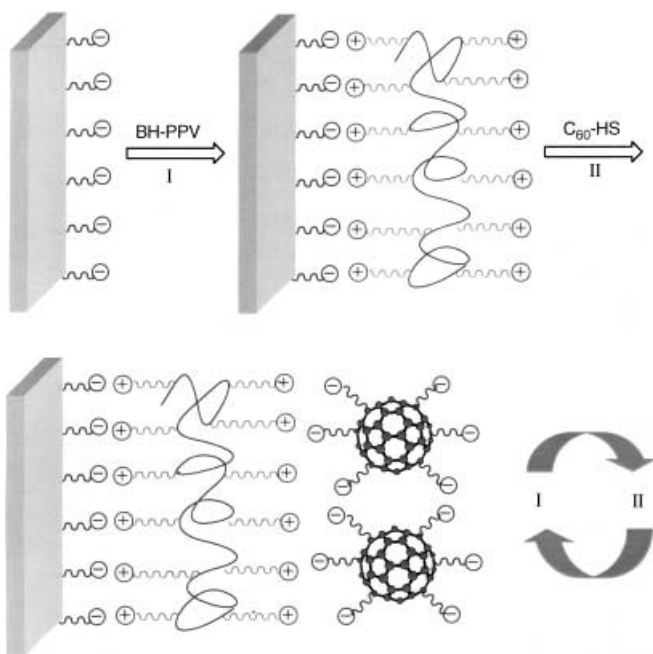
alkoxy benzene was copolymerized with 1,4-divinylbenzene under the standard Heck reaction conditions. The polymerization was easily carried out in DMF in the presence of a catalytic amount (2% mol) of $[Pd(OAc)_2]$ with the tertiary amine and triarylphosphane under an argon atmosphere.^[23] The resulting polymer is well soluble in aqueous solution, owing to the quaternized amine-terminated groups attached to the main chain of BH-PPV. Gel permeation chromatography (GPC) analysis shows that the BH-PPV has an M_w of 13798, M_n of 12776, and M_z of 15267, with M_w/M_n of 1.08. The photophysical characteristics of BH-PPV were investigated in aqueous solution. The π - π^* absorption was observed at $\lambda_{max} = 441$ nm, which is red shifted relative to the value of 400 nm for unsubstituted PPV. The PL spectrum in aqueous solution shows a strong green emission around 519 nm.



Scheme 1. Synthetic route for BH-PPV.

Film growth and characterization: Layer by layer deposition was carried out by sequential treatment of the substrate with solutions of positively charged BH-PPV and negatively charged C_{60} -HS (Scheme 2). The growth of film was monitored by UV/Vis spectroscopy.

Figure 1 shows the absorption spectra of a BH-PPV/ C_{60} -HS multilayer film prepared on a quartz slide. The spectra exhibit a clear absorption around 431 nm,^[24] which is the characteristic band of BH-PPV. In aqueous solution, the π - π^* absorption was observed at $\lambda_{max} = 441$ nm.^[23,25] The 10 nm blue shift for the absorption of the multilayer is probably due to the strong interaction between individual molecules in the densely packed films. In addition, the shift in the absorption maximum of BH-PPV on going from solution to a solid film is caused to a certain extent by the conformational changes that polymer main chains undergo in the deposition and dipping process. The spectra in Figure 1 also ex-



Scheme 2. Fabrication of multilayer assemblies by consecutive absorption of BH-PPV and C₆₀-HS.

hibit two of the major fullerene core transitions at 212 nm and a set of broad shoulders at 280 and 330 nm. These are in excellent agreement with the transitions seen in solution. The insert plot depicts the absorption intensity at 431 nm versus the number of bilayers. A linear fit yields an average increase of the absorption intensity of 0.0075 (correlation coefficient $R = 0.999$) per layer, indicating a stepwise and regular growth process.

Further evidence for the multilayer structure is provided by the small-angle X-ray diffraction study. Figure 2 shows the X-ray diffraction pattern of a seven-bilayer film of BH-PPV and C₆₀-HS prepared on a quartz substrate. The X-ray curves reveal a series of Kiessig fringes, which suggested that the BH-PPV/C₆₀-HS layer-by-layer film is uniform and flat. The total thickness of the film was calculated to be about 14.7 nm from the spacing of the peaks. Since the UV/

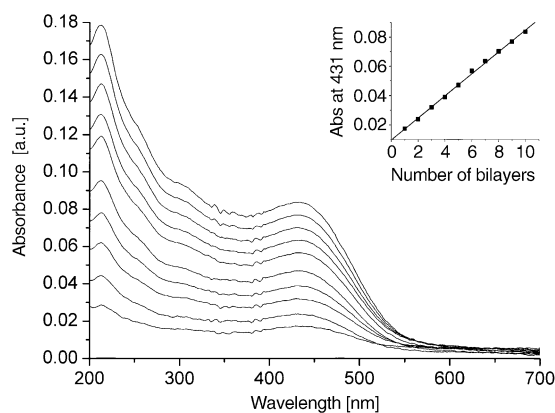


Figure 1. Absorption spectra of BH-PPV/C₆₀-HS multilayer film with different numbers of bilayers. Inset: the relationship of the absorbance and the number of bilayers.

Vis spectra demonstrated that the thickness of the film increased uniformly with the number of layers, the thickness of one bilayer can be calculated to be about 21 Å. The layer-by-layer pattern of the film growth can be clearly seen in the images (not shown) obtained by atomic force microscopy (AFM). The morphologies of the BH-PPV and BH-PPV/C₆₀-HS layers as observed in AFM images are significantly different. The first layer of BH-PPV showed a feature of densely packed nanoparticles having a well-defined spherulike shape with a height variation of about 3 nm. Adsorption of a layer of C₆₀-HS onto the BH-PPV film manifested itself in the formation of a relatively smooth surface with a height variation of about 1 nm. Self-assembly of the C₆₀-HS layer to form the bilayer film decreased the height variation to about 2 nm. It is concluded that the roughness variation of the bilayer of BH-PPV and C₆₀-HS leads to morphological change in comparison to the surface of pure BH-PPV monolayer. The morphologies of the BH-PPV/C₆₀-HS film presents a fine-grained structure with an average diameter of 20 nm. The AFM measurement, together with the linear increase of absorption in the UV/Vis experiment and X-ray diffraction study, suggest that the self-assembly of the BH-PPV/C₆₀-HS ultrathin films is rather uniform and is also in good homogeneity. The AFM images of the multilayer films show that deposition of the BH-PPV/C₆₀-HS multilayer films did not result in any major morphological changes in comparison to the first layer and bilayer film.

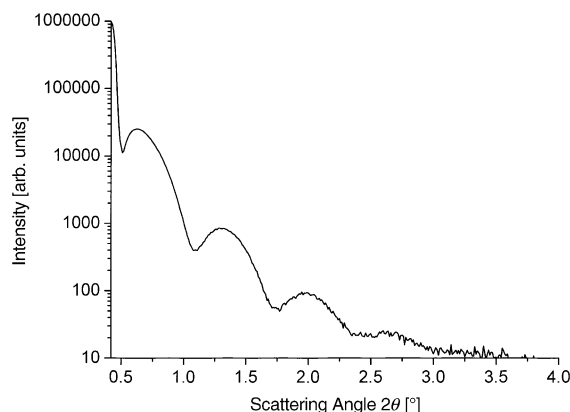


Figure 2. Small-angle X-ray diffraction pattern of a seven-bilayer film of BH-PPV and C₆₀-HS recorded with a modified Bruker D8 diffractometer using CuK α radiation ($\lambda = 1.5405$ Å).

Photocurrent generation: A conventional three-electrode cell was used to measure the photoelectrochemical properties of the self-assembled multilayer film. A platinum wire was used as a counter electrode and the saturated calomel electrode as a reference electrode. A solution of 0.5 M KCl was selected as the supporting electrolyte in all measurements. The indium-tin-oxide (ITO) glass modified with self-assembled multilayer films from 1 to 9-bilayer was used as a working electrode. As a potential application for the multilayer films, we measured the light energy conversion process of the multilayer film. The relationship between photocur-

rent and bilayer number in the self-assembled multilayer films is shown in Figure 3.

We found that the photocurrent increases with increasing bilayer number as long as the film is relatively thin (until the sixth bilayer). The increase in the photocurrent responses indicates that the self-assembled multilayer film is

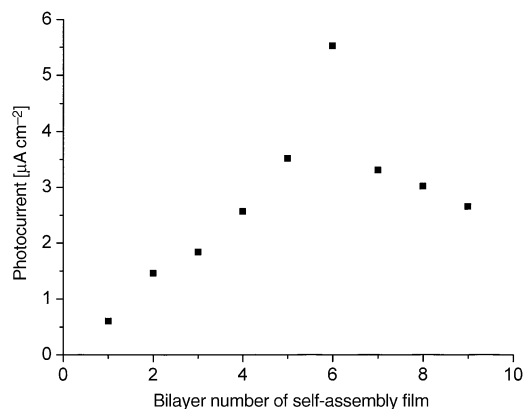


Figure 3. Relationship between photocurrent and layer number of self-assembled multilayer films.

certainly an active species in the photoelectric conversion. As the film gets thicker, the photocurrent shows no steady increase and even decreases. Two factors may contribute to this phenomenon: One is the increasing probability of charge recombination; the other is the increase in the film's electrical resistance with increasing film thickness. Photocurrent generation in the multilayer film is likely the possibility. Organic semiconductor-type behaviour involves photoinduced charge separation within the BH-PPV layer followed by charge separation in the opposite direction. Our results show that the electrostatically linked system features the photocurrent flow from PPV units \rightarrow C_{60} units \rightarrow electrode.^[3h] Repeated photoexcitation of the multilayer films did not result in a decrease in the photocurrent over several hours of alternating light/dark cycles.

The photocurrent generation of six-bilayer BH-PPV and C_{60} -HS film deposited onto an ITO electrode was measured at 7.5 mW cm^{-2} white light irradiation. A steady and rapid cathodic $5.5 \mu\text{A cm}^{-2}$ photocurrent response was produced (Figure 4) as the irradiation of the multilayer film was switched on and off. Importantly, the response to on/off cycling is prompt and reproducible; four cycles are shown in Figure 4. The photocurrent stability in the system was rather good during the monitored time.

Figure 5 shows the photocurrent in the system upon application of different bias potential at the electrode. From Figure 5, we determined that the photocurrent increases with increasing negative bias potential, and decreases with increasing positive bias potential. This indicates that electrons are transferred to the electrolyte through the self-assembled multilayer film from the modified ITO electrode, and when a negative bias potential is applied to the ITO electrode, it can promote electron transfer through this mechanism.

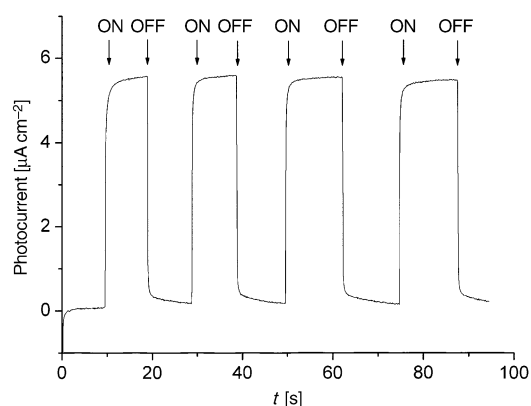


Figure 4. Photocurrent generation of the six-layer BH-PPV/ C_{60} -HS film upon the irradiation of 7.5 mW cm^{-2} white light in 0.5 M KCl solution, no bias voltage is applied.

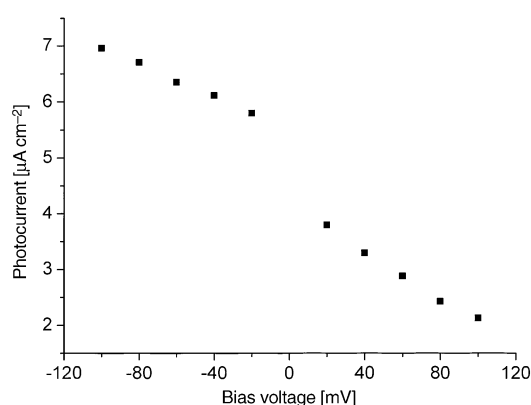


Figure 5. Effect of bias potential on the photocurrent generation of the six-layer BH-PPV/ C_{60} -HS film upon the irradiation of 7.5 mW cm^{-2} white light in 0.5 M KCl solution.

With a change of the excitation wavelengths to the 390–540 nm range, a photocurrent action spectrum is obtained (Figure 6), which is close to the absorption maximum in the investigated wavelength range. The action spectrum shows a typical peak around 430 nm, which corresponds to the BH-PPV in the absorption spectrum. The fact that these two spectra are similar in shape indicates that the photocurrent generation can be attributed to the excitation of BH-PPV incorporated in the BH-PPV/ C_{60} -HS multilayers. The close match of the action and absorption spectra of the modified electrodes suggests that the BH-PPV/ C_{60} -HS multilayer film is responsible for the generation of the observed photocurrent.

Mechanism of photoinduced electron transfer: In order to understand the electron transfer process for the generation of the photocurrent, the energies of the relevant electronic states must be known. Cyclic voltammetry and UV/Vis absorption spectroscopy were used to study the electrochemical behaviour and photophysical characteristics of the compounds described here, allowing us to estimate their relative HOMO and LUMO energies. The oxidation process corresponds to the removal of electrons from the HOMO band,

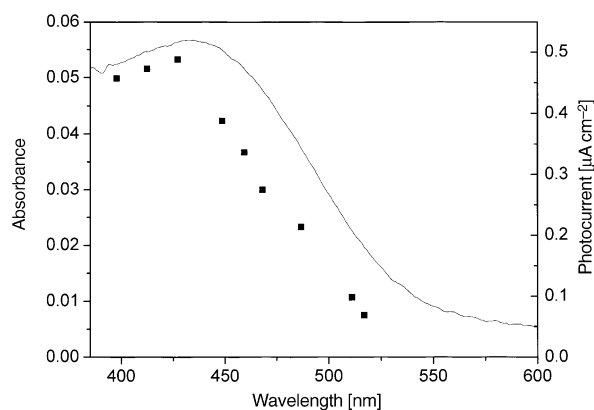


Figure 6. Action (■) and absorption spectra of six-layer BH-PPV/ C_{60} -HS self-assembled film on ITO substrate. The intensities of different wavelengths were all normalized.

whereas the reduction cycle corresponds to the filling of electrons into the LUMO band. Therefore, the onset oxidation and reduction potentials are closely related to energies of the HOMO and LUMO levels of an organic molecule and can provide important information regarding the magnitude of the energy gap. The LUMO levels of BH-PPV and C_{60} -HS are at -1.57 V and -0.59 V versus Ag wire, respectively. The onset oxidation potential of BH-PPV is at 0.65 V versus Ag wire. The HOMO and LUMO values are calculated by assuming the energy level of Ag wire to be at -4.39 eV.^[26] The band gap can be derived from the difference between the onset of the first oxidation potential and the onset of the first reduction potential. In addition, the optical band gap can be estimated from the onset wavelength (λ_{onset}) of the absorption spectrum ($E_g = 1240/\lambda_{\text{onset}}$). Therefore, the optical E_g value of the polymer is 2.26 eV. This result agrees well with the electrochemical energy gap (2.22 eV). The energy of the conduction band of ITO is estimated at -4.5 eV (~ -0.23 V vs Ag wire)^[27] Figure 7 shows a simplified picture of the photoinduced electron pathway for the observed photocurrent. Electrons transfer from the conduction band (CB) of ITO to the donor layer. Upon illumination, the excitons form in this layer. Electron transfer from BH-PPV to C_{60} -HS then occurs, forming a charged-separated state. The C_{60} -HS $^{\cdot-}$ moiety in the charged-separated state gives an electron to an electron carrier such as O_2 ($O_2/O_2^{\cdot-} = -0.46$ V)^[28,29] in the electrolyte solution, and the electrons flow from ITO through the self-assembled multilayer film to the electrolyte, resulting in the observed cathodic photocurrent. It should be noted that the electrochemistry experiment was carried out in DMF solution and the photocurrent was generated in aqueous solution.

We measured the absorption spectra of BH-PPV with and without C_{60} -HS. Comparing the absorption of BH-PPV/ C_{60} -HS, C_{60} -HS, and BH-PPV, it can be seen that the absorption profile and intensity of the mixture are similar to those of the sum of BH-PPV and C_{60} -HS, which shows that no new complex is formed between BH-PPV and C_{60} -HS in the ground state. Actually, the peculiarities of luminescence quenching may reflect some sophisticated details of the charge-transfer process from photoexcited BH-PPV to the

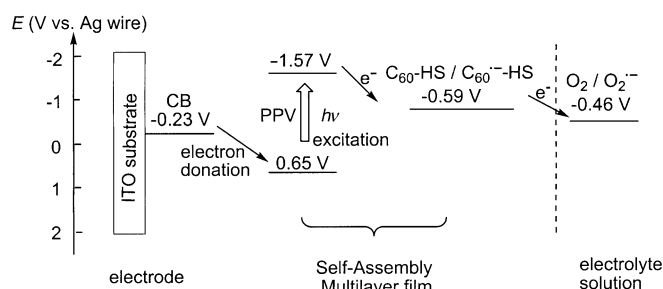


Figure 7. Schematic illustration of cathodic photocurrent generation

quencher molecules. It is well known that C_{60} and its derivatives are good electron acceptors. Figure 8 shows the changes in the fluorescence spectra of BH-PPV with increasing concentration of C_{60} -HS. It is found that a new band with an isoemission point occurs in the long-wavelength region. The dependence of the fluorescence intensity of BH-PPV without C_{60} -HS (F_0) to that with C_{60} -HS (F) on the concentration of C_{60} -HS follows the Stern–Volmer equation [Eq. (1)],^[30] in which τ_0 is the mean lifetime (0.6 ns) of BH-PPV without C_{60} -HS; K_q is the constant ($1.5 \times 10^{15} \text{ M}^{-1} \text{ s}^{-1}$) of the bimolecular quenching.

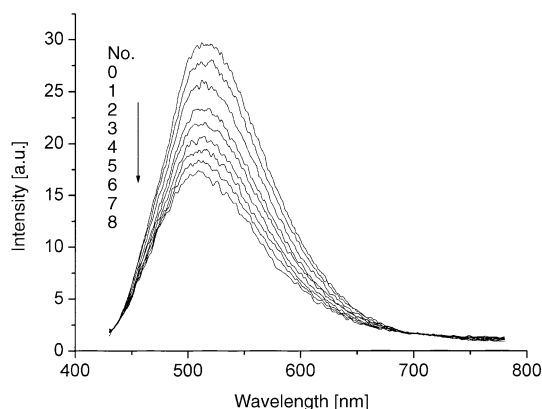


Figure 8. The fluorescence spectra of BH-PPV (1.0×10^{-5} M) in aqueous solution with increasing concentration of C_{60} -HS ($\times 10^{-7}$ M): 0.0 (0), 1.0 (1), 2.0 (2), 3.0 (3), 4.0 (4), 5.0 (5), 6.0 (6), 7.0 (7), 8.0 (8). Excitation wavelength: 410 nm.

$$F_0/F = 1 + K_q \tau_0 [C_{60}\text{-HS}] \quad (1)$$

The fluorescence quenching experiment reflects the charge-transfer process indirectly. However, the ESR experiment can also show us this process directly. The ESR spectra of the mixture of BH-PPV and C_{60} -HS in aqueous solution are shown in Figure 9. An ESR signal appears after irradiation of the mixture at a wavelength of about 450 nm for 15 min. This is in agreement with other groups' results.^[31] The experiment was done in an aqueous solution of BH-PPV without C_{60} -HS under the same conditions and no signal was observed. The ESR results confirmed the formation of C_{60} -HS $^{\cdot-}$ by the irradiation of light.

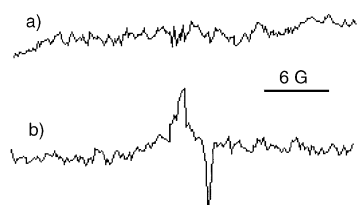


Figure 9. ESR spectra of the C_{60} anion radical after irradiation of BH-PPV (1.0×10^{-5} M) in aqueous solution without (a) and with C_{60} -HS (b) (8.0×10^{-7} M).

Conclusion

The proposed approach provides a new avenue for producing materials for photovoltaic conversion systems, and layer-by-layer deposition can be used as a viable alternative for the fabrication of a controllable molecular array for efficient energy and electron transfer. Interestingly, our approach may provide a useful and easy way to directly fabricate photovoltaic devices. We believe that the photoactive films will be useful in solar energy conversion, as well as optical and optical limiting applications. Thus, this work provides a significant result for future organization of photodriven single-electron-transfer devices.

Experimental Section

General methods: The Gel permeation chromatography (GPC) measurements were performed on a PL-GPC-210 chromatograph at 35 °C using DMF as eluant. The molecular weight and the molecular weight distribution were calculated on the basis of monodispersed polystyrene standards. The ^1H NMR spectra were collected on a Bruker DMX-300 spectrometer (SiMe_4). Mass spectra were obtained on the VG-ZAB-HS (EI) spectrometer. FT-IR spectra were measured on a Bruker EQUINOX55 spectrometer. The UV/Vis and fluorescence spectra were obtained on a Hitachi U-3010 and Hitachi F-4500 spectrometer, respectively. Elemental analyses were carried out on the Carlo-Erba 1160 elemental analyzer. Thermal analysis was performed by using the Perkin-Elmer DSC-7 and TGA-7 systems with heating rates of 20°Cmin^{-1} under a nitrogen atmosphere. Small-angle X-ray diffraction was carried out with a high-resolution Bruker D8 diffractometer using $\text{CuK}\alpha$ radiation ($\lambda = 1.5405 \text{ \AA}$). Atomic force microscopy (AFM) measurements were carried out in air at room temperature with a Nanoscope IIIa instrument (Digital Instruments) operating in tapping mode. AFM images shown were taken on mica substrates.

Materials: 1,4-Bis(3-bromotrimethylammonio)propoxy)-2,5-diiodobenzene (2),^[32] 1,4-bis[2-(2-hydroxyethoxy)ethoxy]-2,5-diiodobenzene (3),^[33] and the sodium salt of hexa(sulfobutyl)fullerenes^[34] were prepared according to literature procedures. DMF was purified by distillation over phosphorus pentoxide and triethylamine was distilled over CaH_2 before use. Dialysis membranes with a 3500 cut-off were used for the purification of the polymer after precipitation from acetone.

The quartz slides for the UV/Vis study were cleaned by sonication in isopropyl alcohol for 1 h, and subsequently dried with argon. Slides were dipped in 5 N KOH for 30 s, rinsed with deionized water to remove residual KOH, and then dried under argon to obtain substrates with a negatively charged surface. The quartz substrate for the small-angle X-ray diffraction study was cleaned with a solution of three volumes of H_2SO_4 and one volume of 30% H_2O_2 for 30 min and washed with deionized water. After drying, the slide was treated with 5% (v/v) (3-aminopropyl)triethoxysilane (Aldrich) in anhydrous toluene at 105 °C for 15 h under an atmosphere of dry nitrogen. The amine-functionalized slide was washed with toluene, methanol, deionized water and dried. Then the substrate was immersed in a solution containing C_{60} -HS (10 mg), HCl (0.1 N,

0.5 mL), and deionized water (9.5 mL), in order to protonate the amino groups. Deionized water used in all experiments and cleaning steps had a resistivity higher than $18 \text{ M}\Omega\text{ cm}$.

Synthesis of 1,4-bis[2-(2-hydroxyethoxy)ethoxy]-2,5-divinylbenzene (4): A mixture of compound 3 (0.538 g, 1 mmol), vinyl tributyltin (0.634 g, 2 mmol), and $[\text{Pd}(\text{PPh}_3)_4]$ (0.046 g, 0.04 mmol) in DMF (8 mL) was stirred at 100 °C for 5 h. After cooling to room temperature, the mixture was filtered, and the filtrate was poured into water. After extraction with dichloromethane, the organic layer was collected and dried over MgSO_4 . The solvent was then removed and the residue was purified by column chromatography. Elution with 5% CH_3OH in CH_2Cl_2 resulted in compound 4 as a yellow solid (0.18 g, 53%). M.p. 57–59 °C; ^1H NMR (300 MHz, CDCl_3 , TMS): $\delta = 3.67$ (m, 4H; OCH_2 -), 3.75 (m, 4H; OCH_2 -), 3.86 (m, 4H; OCH_2 -), 4.15 (m, 4H; OCH_2 -), 5.27 (d, 2H; vinyl proton), 5.73 (d, 2H; vinyl proton), 6.99 (t, 2H; vinyl proton), 7.05 (s; aromatic protons); MS (70 eV): m/z : 338 $[\text{M}]^+$; elemental analysis calcd (%) for $\text{C}_{18}\text{H}_{26}\text{O}_6$: C 63.91, H 7.69; found: C 63.58, H 7.41.

Synthesis of the BH-PPV:^[25] A mixture of compound 2 (144 mg, 0.2 mmol), compound 4 (69 mg, 0.204 mmol), $[\text{Pd}(\text{OAc})_2]$ (1.8 mg, 0.008 mmol), tri-*o*-tolylphosphane (12 mg, 0.04 mmol), triethylamine (70 μL), and DMF (5 mL) was stirred at 80 °C overnight under argon. The hot solution was poured into 200 mL of acetone and the polymer precipitated. The collected precipitate was dissolved in doubly distilled water, filtered, and the solution was dialyzed using a membrane with a 3500 cut-off for 2 d (8 water changes). The water was evaporated, yielding the product as a dark red solid (69 mg, 43%). ^1H NMR (300 MHz, D_2O , TMS): $\delta = 1.93$ (br, 4H; $-\text{CH}_2-$), 2.65–2.98 (br, 22H; $-\text{N}-\text{CH}_2-$, $-\text{N}-\text{CH}_2-$), 3.31–4.09 (m, 20H; $-\text{OCH}_2$), 7.05 (br, 4H; vinyl proton), 7.45 (br, 4H; aromatic protons); FT-IR (KBr pellet): 3030, 2926, 2873, 1205, 968 cm^{-1} ; GPC (DMF): M_w 13798, M_n 12776, M_z 15267, PDI 1.08; elemental analysis calcd (%) for $\text{C}_{36}\text{H}_{56}\text{Br}_2\text{N}_2\text{O}_8$: C 53.87, H 6.98; found: C 52.55, H 6.85.

Preparation of the layer-by-layer films: The fabrication of the multilayer films was carried out according to the following steps. The cleaned substrates were immersed alternately in PDPA solution and in the C_{60} -HS solution for 5 min for each deposition. Both solution concentrations were fixed at 1 mg mL^{-1} . After each adsorption step, the surface of the self-assembled film was washed with deionized water and dried with a stream of argon gas. All of the experiments were carried out at room temperature.

Electrochemical measurements: Cyclic voltammograms (CV) were recorded on an IM 6e Zahner Potentiostat. Dried DMF was used to prepare a solution of BH-PPV (4×10^{-4} M) and C_{60} -HS (5×10^{-5} M) containing Bu_4NPF_6 (0.1 M) as a supporting electrolyte. The scan rates of BH-PPV and C_{60} -HS were 20 mV s^{-1} and 200 mV s^{-1} , respectively. A three-electrode configuration consisting of a glassy carbon working electrode, a Pt wire counter electrode, and an Ag wire quasi-reference electrode was used. All potentials reported are referenced versus Ag wire. N_2 bubbling was used to remove oxygen from the electrolyte solutions in the electrochemical cell.

Photoelectrochemical measurements: The photocurrent measurements were carried out on a model 600 voltammetric analyzer (CH Instruments, USA), and a 500 W xenon lamp was used as the light source. The intensities of incident beams were checked by a power and energy meter (Model 372, Scientech). The IR light was filtered throughout the experiments with a Toshiba IRA-25S filter (Japan) to protect the electrodes from heating.

Substrates were unmodified ITO glass and were cleaned using an ultrasonic bath in isopropyl alcohol, then deionized water, prior to use. The sheet resistance was $\sim 15 \Omega$ per square.

Fluorescence lifetime measurements: Fluorescence decay was measured by the time-resolved streak camera (Hamamatsu C2909) method. The instrument response function was about 30 ps. The software used to fit the fluorescence decay curves was compiled based on Matlab 5.2 (Mathworks).

Electron spin resonance measurements: The ESR experiments were performed on a Bruker ESP-300 spectrometer with the X-band. A halogen lamp was used as the irradiation source with emission monochromaticity at a wavelength of about 450 nm. The ESR spectrometer settings were as follows: sweep width 30 G, microwave power 12.9×10^{-3} W, modulation

amplitude 1.0 G, receiver gain 7.96×10^5 , time constant 1.3107 s, centre field 3360 G. The solution of BH-PPV and C₆₀-HS was deaerated with a nitrogen stream prior to irradiation.

Acknowledgement

This work was supported by the Major State Basic Research Development Program and the National Natural Science Foundation of China (20151002, 90101025).

- [1] a) S. W. Keller, S. A. Johnson, E. S. Brigham, E. H. Yonemoto, T. E. Mallouk, *J. Am. Chem. Soc.* **1995**, *117*, 12879–12880; b) B. Choudhury, A. C. Weedon, J. R. Bolton, *Langmuir* **1998**, *14*, 6192–6198; c) D. Gust, T. A. Moore, A. L. Moore, *Acc. Chem. Res.* **2001**, *34*, 40–48; d) E. V. Pletneva, M. M. Crnogorac, N. M. Kostic, *J. Am. Chem. Soc.* **2002**, *124*, 14342–14354; e) B. Pispisa, M. Venanzi, L. Stella, A. Paleschi, G. Zanotti, *J. Phys. Chem. B* **1999**, *103*, 8172–8179; f) Z. F. Dai, L. Dähne, E. Donath, H. Möhwald, *Langmuir* **2002**, *18*, 4553–4555; g) M. L. A. Abrahamsson, H. B. Baudin, A. Tran, C. Philouze, K. E. Berg, M. K. Raymond-Johansson, L. C. Sun, B. Åkermarck, S. Styring, L. Hammarstrom, *Inorg. Chem.* **2002**, *41*, 1534–1544; h) F. B. Abdelrazzaq, R. C. Kwong, M. E. Thompson, *J. Am. Chem. Soc.* **2002**, *124*, 4796–4803.
- [2] a) *The Photosynthetic Reaction Center* (Eds.: J. Deisenhofer, J. R. Norris), Academic Press, San Diego, **1993**; b) G. McDermott, S. M. Prince, A. A. Freer, A. M. Hawthornwaite-Lawless, M. Z. Papiz, R. J. Cogdell, N. W. Isaacs, *Nature* **1995**, *374*, 517–521; c) H. Imahori, H. Norieda, H. Yamada, Y. Nishimura, I. Yamazaki, Y. Sakata, S. Fukuzumi, *J. Am. Chem. Soc.* **2001**, *123*, 100–110; d) G. Kodis, P. A. Liddell, L. de la Garza, P. C. Clausen, J. S. Lindsey, A. L. Moore, T. A. Moore, D. Gust, *J. Phys. Chem. A* **2002**, *106*, 2036–2048; e) K. G. Thomas, V. Biju, D. M. Guldi, P. V. Kamat, M. V. George, *J. Phys. Chem. B* **1999**, *103*, 8864–8869; f) K. G. Thomas, V. Biju, D. M. Guldi, P. V. Kamat, M. V. George, *J. Phys. Chem. A* **1999**, *103*, 10755–10763.
- [3] a) J. W. Verhoeven, in *Electron Transfer* (Eds.: J. Jortner, M. Bixon), Wiley, New York, **1999**, Part 1; b) G. Zerza, A. Cravino, H. Neugebauer, N. S. Sariciftci, R. Gomez, J. L. Segura, N. Martin, M. Svensson, M. R. Andersson, *J. Phys. Chem. A* **2001**, *105*, 4172–4176; c) F. D'Souza, G. R. Deviprasad, M. S. Rahman, J. P. Choi, *Inorg. Chem.* **1999**, *38*, 2157–2160; d) N. V. Tkachenko, L. Rantala, A. Y. Tauber, J. Helaja, P. H. Hynninen, H. Lemmetyinen, *J. Am. Chem. Soc.* **1999**, *121*, 9378–9387; e) H. Imahori, H. Yamada, Y. Nishimura, I. Yamazaki, Y. Sakata, *J. Phys. Chem. B* **2000**, *104*, 2099–2108; f) N. P. Redmore, I. V. Rubtsov, M. J. Therien, *Inorg. Chem.* **2002**, *41*, 566–570; g) D. M. Guldi, S. Gonzalez, N. Martin, A. Anton, J. Garin, J. Orduna, *J. Org. Chem.* **2000**, *65*, 1978–1983; h) A. Ikeda, T. Hatano, S. Shinkai, T. Akiyama, S. Yamada, *J. Am. Chem. Soc.* **2001**, *123*, 4855–4856; i) P. V. Kamat, S. Barazzouk, S. Hotchandani, K. G. Thomas, *Chem. Eur. J.* **2000**, *6*, 3914–3921.
- [4] a) P. Seta, E. Bienvenue, A. Moore, P. Mathis, R. Bensasson, P. Liddell, P. Pessiki, A. Joy, T. Moore, *Nature* **1985**, *316*, 653; b) Y. Sakata, H. Tatemitsu, E. Bienvenue, P. Seta, *Chem. Lett.* **1988**, 1625–1628; c) K. C. Hwang, D. Mauzerall, *Nature* **1993**, *361*, 138–140; d) K. Sun, D. Mauzerall, *J. Phys. Chem. B* **1998**, *102*, 6440–6447.
- [5] a) A. Slama-Schwok, M. Ottolenghi, D. Avnir, *Nature* **1992**, *355*, 240–242; b) R. E. Sassoan, S. Gershuni, J. Rabani, *J. Phys. Chem.* **1992**, *96*, 4692–4698.
- [6] a) M. Fujihira, M. Sakomura, *Thin Solid Films* **1989**, *179*, 471–476; b) M. Sakomura, M. Fujihira, *Thin Solid Films* **1996**, *273*, 181–184; c) Y. L. Zhao, L. B. Gan, D. J. Zhou, C. H. Huang, J. Z. Jiang, W. Liu, *Solid State Commun.* **1998**, *106*, 43–48; d) B. O'Beirn, V. Casey, M. A. Gubbins, J. B. McMonagle, *Thin Solid Films* **1998**, *327*, 652–654.
- [7] a) A. Shah, P. Torres, R. Tscharnner, N. Wyrsh, H. Keppner, *Science* **1999**, *285*, 692–698; b) K. Uosaki, T. Kondo, X. Q. Zhang, M. Yanagida, *J. Am. Chem. Soc.* **1997**, *119*, 8367–8368; c) J. L. Snover, H. Byrd, E. P. Suponeva, E. Vicenzi, M. E. Thompson, *Chem. Mater.* **1996**, *8*, 1490–1499; d) A. Ulman, *Introduction to Ultrathin Organics Films: From Langmuir-Blodgett to Self-assembly*, Academic Press, Boston, **1991**; e) Y. T. Tao, C. C. Wu, J. Y. Eu, W. L. Lin, *Langmuir* **1997**, *13*, 4018–4023; f) T. Kondo, M. Yanagida, S. Nomura, T. Ito, K. Uosaki, *J. Electroanal. Chem.* **1997**, *438*, 121–126.
- [8] a) G. Cao, H. G. Hong, T. E. Mallouk, *Acc. Chem. Res.* **1992**, *25*, 420–427; b) E. Katz, *Chem. Mater.* **1994**, *6*, 2227–2232; c) M. Thompson, *Chem. Mater.* **1994**, *6*, 1168–1175.
- [9] a) G. Decher, J. D. Hong, J. Schmitt, *Thin Solid Films* **1992**, *210–211*, 831–835; b) Y. Lvov, G. Decher, H. Möhwald, *Langmuir* **1993**, *9*, 481–486; c) G. Decher, Y. Lvov, J. Schmitt, *Thin Solid Films* **1994**, *244*, 772–777; d) G. Decher, *Science* **1997**, *277*, 1232–1237.
- [10] G. Z. Mao, Y. H. Tsao, M. Tirrell, H. T. Davis, V. Hessel, H. Ringsdorf, *Langmuir* **1995**, *11*, 942–952.
- [11] a) M. Lahav, V. Heleg-Shabtai, J. Wasserman, E. Katz, I. Willner, H. Dürr, Y. Z. Hu, S. H. Bossmann, *J. Am. Chem. Soc.* **2000**, *122*, 11480–11487; b) C. P. Luo, D. M. Guldi, M. Maggini, E. Menna, S. Mondini, N. A. Kotov, M. Prato, *Angew. Chem.* **2000**, *112*, 4052–4056; *Angew. Chem. Int. Ed.* **2000**, *39*, 3905–3909; c) D. M. Guldi, F. Pellarini, M. Prato, C. Granito, L. Troisi, *Nano Lett.* **2002**, *2*, 965–968.
- [12] a) M. Lösche, J. Schmitt, G. Decher, W. G. Bouwman, K. Kjaer, *Macromolecules* **1998**, *31*, 8893–8906; b) S. T. Dubas, J. B. Schlenoff, *Macromolecules* **1999**, *32*, 8153–8160; c) V. Pardo-Yissar, E. Katz, O. Lioubashevski, I. Willner, *Langmuir* **2001**, *17*, 1110–1118; d) C. A. Cutler, M. Bouguettaya, J. R. Reynolds, *Adv. Mater.* **2002**, *14*, 684–688; e) L. Zhai, R. D. McCullough, *Adv. Mater.* **2002**, *14*, 901–905; f) E. Vazquez, D. M. Dewitt, P. T. Hammond, D. M. Lynn, *J. Am. Chem. Soc.* **2002**, *124*, 13992–13993; g) J. F. Hicks, Y. Seok-Shon, R. W. Murray, *Langmuir* **2002**, *18*, 2288–2294; h) M. L. Bruening, D. M. Sullivan, *Chem. Eur. J.* **2002**, *8*, 3833–3837.
- [13] a) J. W. Ostrander, A. A. Mamedov, N. A. Kotov, *J. Am. Chem. Soc.* **2001**, *123*, 1101–1110; b) Y. M. Lvov, J. F. Rusling, D. L. Thomsen, F. Papadimitrakopoulos, T. Kawakami, T. Kunitake, *Chem. Commun.* **1998**, 1229–1230; c) K. M. Chen, X. P. Jiang, L. C. Kemmerling, P. T. Hammond, *Langmuir* **2000**, *16*, 7825–7834; d) E. W. L. Chan, D. C. Lee, M. K. Ng, G. H. Wu, K. Y. C. Lee, L. P. Yu, *J. Am. Chem. Soc.* **2002**, *124*, 12238–12243; e) E. C. Hao, T. Q. Lian, *Chem. Mater.* **2000**, *12*, 3392–3396; f) J. Schmitt, G. Decher, W. J. Dressick, S. L. Brandow, R. E. Geer, R. Shashidhar, J. M. Calvert, *Adv. Mater.* **1997**, *9*, 61.
- [14] a) B. van Duffel, R. A. Schoonheydt, C. P. M. Grim, F. C. De Schryver, *Langmuir* **1999**, *15*, 7520–7529; b) Y. Lvov, K. Ariga, I. Ichinose, T. Kunitake, *Langmuir* **1996**, *12*, 3038–3044; c) A. Mamedov, J. Ostrander, F. Aliev, N. A. Kotov, *Langmuir* **2000**, *16*, 3941–3949.
- [15] a) D. Wöhrle, D. Meissner, *Adv. Mater.* **1991**, *3*, 129–138; b) W. A. Nevin, G. A. Chamberlain, *J. Appl. Phys.* **1991**, *69*, 4324–4332; c) G. D. Sharma, S. C. Mathur, D. C. Dube, *J. Mater. Sci.* **1991**, *26*, 6547–6552; d) J. Danziger, J. P. Dodelet, P. Lee, K. M. Nebesny, N. R. Armstrong, *Chem. Mater.* **1991**, *3*, 821–829; e) J. Takada, H. Awaji, M. Koshioka, A. Nakajima, W. A. Nevin, *Appl. Phys. Lett.* **1992**, *61*, 2184–2186.
- [16] N. S. Sariciftci, L. Smiowitz, A. J. Heeger, F. Wudl, *Science* **1992**, *258*, 1474–1476.
- [17] a) H. W. Kroto, J. R. Heath, S. C. O'Brien, R. F. Curl, R. E. Smalley, *Nature* **1985**, *318*, 162; b) W. Krätschmer, L. D. Lamb, K. Fostiropoulos, D. R. Huffman, *Nature* **1990**, *347*, 354–358; c) *Science of Fullerenes and Carbon Nanotubes*, M. S. Dresslhaus, G. Dresslhaus, P. C. Eklund, Academic Press, San Diego, **1996**; d) F. Diederich, C. Thilgen, *Science* **1996**, *271*, 317–323; e) A. Hirsch, *Fullerenes and Related Structure, Topics in Current Chemistry, Vol. 199*, Springer, Berlin, **1999**; f) J. L. Segura, N. Martin, *J. Mater. Chem.* **2000**, *10*, 2403–2435; g) M. Prato, *J. Mater. Chem.* **1997**, *7*, 1097–1109; h) B. Z. Tang, H. Y. Xu, J. W. Y. Lam, P. P. S. Lee, K. T. Xu, Q. H. Sun, K. K. L. Cheuk, *Chem. Mater.* **2000**, *12*, 1446–1455; i) *Fullerenes: Chemistry, Physics and Technology*, (Eds.: K. Kadish, R. Ruoff), Wiley, **2000**; j) A. J. Heeger, *J. Phys. Chem. B* **2001**, *105*, 8475–8491; k) *Handbook of Conductive Molecules and Polymers, Vol. 1–4* (Ed.: H. S. Nalwa), Wiley, Chichester, **1997**; l) *Handbook of Conducting Polymers*, 2nd edition (Eds.: T. A. Skotheim, R. L. Elsenbaumer, J. R. Reynolds), Marcel Dekker, New York, **1998**; m) *Semi-*

- conducting Polymers, *Chemistry Physics and Engineering* (Eds.: G. Hadziioannu, P. F. van Hutten), Wiley, Weinheim, **2000**; n) A. Cravino, N. S. Sariciftci, *J. Mater. Chem.* **2002**, *12*, 1931–1943.
- [18] a) Y. J. Liu, Y. X. Wang, H. X. Lu, R. O. Claus, *J. Phys. Chem. B* **1999**, *103*, 2035–2036; b) H. Hong, D. Davidov, C. Kallinger, U. Lemmer, J. Feldmann, E. Harth, A. Gügel, K. Müllen, *Synth. Met.* **1999**, *102*, 1487; c) T. Piok, C. Brands, P. J. Neyman, A. Erlacher, C. Soman, M. A. Murray, R. Schroeder, W. Graupner, J. R. Hefflin, D. Marciu, A. Drake, M. B. Miller, H. Wang, H. Gibson, H. C. Dorn, G. Leising, M. Guzy, R. M. Davis, *Synth. Met.* **2001**, *116*, 343–347.
- [19] a) A. R. Brown, K. Pichler, N. C. Greenham, D. D. C. Bradley, R. H. Friend, P. L. Burn, A. B. Holmes, *Synth. Met.* **1993**, *57*, 4117–4122; b) J. Cornil, D. Beljonne, R. H. Friend, J. L. Bredas, *Chem. Phys. Lett.* **1994**, *223*, 82–88; c) E. K. Miller, C. J. Brabec, H. Neugebauer, A. J. Heeger, N. S. Sariciftci, *Chem. Phys. Lett.* **2001**, *335*, 23–26.
- [20] a) N. Martin, L. Sanchez, B. Illescas, I. Perez, *Chem. Rev.* **1998**, *98*, 2527–2547; b) D. M. Guldi, M. Prato, *Acc. Chem. Res.* **2000**, *33*, 695–703; c) C. A. Reed, R. D. Bolskar, *Chem. Rev.* **2000**, *100*, 1075–1119.
- [21] a) A. C. Fou, O. Onitsuka, M. Ferreira, M. F. Rubner, B. R. Hsieh, *J. Appl. Phys.* **1996**, *79*, 7501–7509; b) O. Onitsuka, A. C. Fou, M. Ferreira, B. R. Hsieh, M. F. Rubner, *J. Appl. Phys.* **1996**, *80*, 4067–4071; c) H. Mattoussi, L. H. Radzilowski, B. O. Dabbousi, E. L. Thomas, M. G. Bawendi, M. F. Rubner, *J. Appl. Phys.* **1998**, *83*, 7965–7974; d) H. Mattoussi, L. H. Radzilowski, B. O. Dabbousi, D. E. Fogg, R. R. Schrock, E. L. Thomas, M. F. Rubner, M. G. Bawendi, *J. Appl. Phys.* **1999**, *86*, 4390–4399; e) A. Wu, D. Yoo, J. K. Lee, M. F. Rubner, *J. Am. Chem. Soc.* **1999**, *121*, 4883–4891.
- [22] H. Mattoussi, M. F. Rubner, F. Zhou, J. Kumar, S. K. Tripathy, L. Y. Chiang, *Appl. Phys. Lett.* **2000**, *77*, 1540–1542.
- [23] Z. N. Bao, Y. M. Chen, R. B. Cai, L. P. Yu, *Macromolecules* **1993**, *26*, 5281–5286.
- [24] a) J. D. Hong, D. Kim, K. Cha, J. Jin, *Synth. Met.* **1997**, *84*, 815–816; b) H. L. Wang, D. W. McBranch, V. I. Klimov, R. Helgeson, F. Wudl, *Chem. Phys. Lett.* **1999**, *315*, 173–180.
- [25] H. M. Li, C. H. Xiang, Y. L. Li, S. Q. Xiao, H. J. Fang, D. B. Zhu, “Polymers-Properties”, presented at *Int. Conf. On Science and Technology of Synthetic Metals 2002 (ICSM 2002)* Shanghai, China, June 28–July 5 **2002**.
- [26] Y. F. Li, Y. Cao, J. Gao, D. L. Wang, G. Yu, A. J. Heeger, *Synth. Met.* **1999**, *99*, 243–248.
- [27] L. Sereno, J. J. Silber, L. Otero, M. del Valle Bohodrquez, A. L. Moore, T. A. Moore, D. Gust, *J. Phys. Chem.* **1996**, *100*, 814–821.
- [28] Y. S. Kim, K. Liang, K. Y. Law, D. G. Whitten, *J. Phys. Chem.* **1994**, *98*, 984–988.
- [29] It is well known that O₂ is vital in the photocurrent generation process.^[28] O₂ bubbling of the electrolyte solution increased the photocurrent by ~20–30% and successive N₂ bubbling of the solution decreased it nearly to the initial state. The results indicate that O₂ is an electron acceptor for cathodic photocurrent generation.
- [30] *Principles of Fluorescence Spectroscopy* (Ed.: J. R. Lakowicz), Plenum, New York, **1993**.
- [31] a) T. Konishi, Y. Sasaki, M. Fujitsuka, Y. Toba, H. Moriyama, O. Ito, *J. Chem. Soc. Perkin Trans. 2* **1999**, 551–556; b) J. L. Yang, F. L. Bai, H. Z. Lin, M. Zhen, Y. P. Zhang, Y. L. Li, J. Sun, Y. Liu, *Macromol. Chem. Phys.* **2001**, *202*, 1824–1828.
- [32] D. T. McQuade, A. H. Hegedus, T. M. Swager, *J. Am. Chem. Soc.* **2000**, *122*, 12389–12390.
- [33] Q. Zhou, T. M. Swager, *J. Am. Chem. Soc.* **1995**, *117*, 12593–12602.
- [34] Y. Chi, J. B. Bhonsle, T. Canteenwala, J. P. Huang, J. Shiea, B. J. Chen, L. Y. Chiang, *Chem. Lett.* **1998**, *5*, 465–466.

Received: April 11, 2003
Revised: August 5, 2003 [F5037]